

Appendix N

Grid Resolution Journal Article

A quantitative assessment of the influence of grid resolution on predictions of future-year air quality in North Carolina, USA

Saravanan Arunachalam^{a,*}, Andrew Holland^a, Bebhinn Do^b,
Michael Abraczinskas^b

^a*Carolina Environmental Program, University of North Carolina at Chapel Hill, Bank of America Plaza, CB #6116, 137 E. Franklin St., Chapel Hill, NC 27599-6116, USA*

^b*Division of Air Quality, North Carolina Department of Environment and Natural Resources, 1641 Mail Service Center, Raleigh, NC 27699-1641, USA*

Received 14 February 2005; received in revised form 5 January 2006; accepted 5 January 2006

Abstract

Increased focus has been directed at fine-scale modeling for improving the ability of air quality modeling systems to capture local phenomena. While numerous studies have investigated model performance at finer resolution (4–5 km), there is relatively limited information available for choosing the optimum grid resolution for predicting future air quality in attainment demonstration studies. We demonstrate an evaluation of the MM5–SMOKE–MAQSIP modeling system for four 8-h ozone episodes in the summers of 1995, 1996 and 1997 in North Carolina using a one-way nested 36/12/4-km application. After establishing acceptable base-case model performance for ozone predictions during each episode, we developed future-year emissions control scenarios for 2007 and 2012, and finally computed relative reduction factors (RRFs) using model outputs from each of the three grid resolutions. Our analyses, based upon qualitative as well as quantitative approaches like the Student's *t*-test, indicate that RRFs computed at specific monitoring locations—and hence predicted future-year air quality—are not very different between the 4- and 12-km results, while the differences are slightly larger between the 4- and 36-km results. The results imply that grid resolution contributes to a variability of about 1–3 ppb in the projected future-year design values; this variability needs to be incorporated into policy-relevant decision-making. Since this assessment was performed for four different episodes under diverse meteorological, physical and chemical regimes, one can generalize the results from this study. They are also relevant for regional modeling applications that are currently ongoing for studying PM_{2.5} nonattainment issues, where the need for annual base-year and future-year simulations for demonstrating attainment may place a large demand on computing resources. Based upon the results from this study, future studies may consider using results from 12-km modeling to address future-year air quality goals for ozone and PM_{2.5} and its components, and then incorporate grid-resolution uncertainties into the computed results.

© 2006 Elsevier Ltd. All rights reserved.

Keywords: Emissions strategies; CMAQ; Student's *t*-test; O₃ NAAQS; Attainment

1. Introduction

In 1997, the US Environmental Protection Agency (US EPA) revised the National Ambient

*Corresponding author. Tel.: +1 919 966 2126;
fax: +1 919 843 3113.

E-mail address: sarav@email.unc.edu (S. Arunachalam).

Air Quality Standard (NAAQS) for ozone from a 1-h-based standard of 0.120 ppm to 0.080 ppm measured over an 8-h period; this is called the 8-h O₃ standard (Federal Register, 1997). The new US NAAQS is met at an ambient air quality monitoring site when the 3-year average of the annual fourth-highest daily maximum 8-h average O₃ concentration is ≤ 0.080 ppm (i.e., the site is said to be in attainment). This revised NAAQS for O₃ is more stringent than the 1-h O₃ standard and more protective of public health. Based upon 8-h O₃ measurements from 2001 to 2003, the US EPA designated a total of 474 counties in the US as not attaining the 8-h O₃ standard in 2004 (Federal Register, 2004). In North Carolina alone, 32 counties were designated nonattainment. The Clean Air Act Amendments of 1990 established selected comprehensive, three-dimensional (3-D) photochemical air quality simulation models as the required regulatory tools for analyzing the urban and regional problem of high ambient O₃ levels across the US (US EPA, 1991). These models are currently applied to study and establish strategies for meeting the NAAQS for O₃ nonattainment areas, and State Implementation Plans resulting from these efforts must be submitted to the US EPA. The US EPA has developed a draft modeling guidance document (US EPA, 1999) for demonstrating attainment of the NAAQS for 8-h O₃. In this document, the US EPA recommends a methodology for applying air quality models to generate predictions that indicate whether a given set of emissions controls is likely to demonstrate attainment in the future. This involves establishing acceptable base-case model performance for the area of interest, then using the same system to model future-year emissions reductions strategies to test for attainment.

With this background, the use of grid-based photochemical models has expanded dramatically to include spatial scales varying from urban to regional. Users selecting a modeling system for a given application need to fully understand the structural and algorithmic differences between models and of their possible impacts on both operational and scientific inferences that may be drawn from the models' respective simulations (Russell and Dennis, 2000). These differences could significantly affect the development of emissions control strategies for attaining the O₃ NAAQS. Sillman et al. (1990) suggest that degrading the model horizontal resolution can cause a systematic positive bias in O₃ simulation, since the artificial

dilution of NO_x emissions over relatively large grid volumes can increase the O₃ production efficiency per unit of NO_x oxidized (Liu et al., 1987). Similar positive bias in predicted O₃ resulting from degradation of horizontal grid resolution has been reported in simulations over southern California by Kumar et al. (1994). Jang et al. (1995a, b) showed that grid resolution significantly influences both rates of chemistry and vertical transport processes, and that coarser grids tend to underpredict ozone maxima over major source areas. Through box-model calculations of O₃ production efficiency for a variety of conditions, Liang and Jacobson (2000) suggest that coarsely resolved models might underpredict or overpredict O₃ production because they are unable to accurately represent the blending of air masses of different origins. Recently, an operational assessment of the application of the draft guidance in demonstrating attainment of the O₃ NAAQS has shown that one needs to account for model-to-model uncertainty in the attainment demonstration (Sistla et al., 2004). The authors demonstrate that the choice of modeling system may bring an area into attainment or not, depending upon the estimated response of the chosen modeling system. Here, we present a case that the choice of grid resolution also needs to be judiciously made, as the results from our future-year modeling show different sites being in attainment or non-attainment of the O₃ NAAQS depending upon the chosen model grid resolution.

2. Modeling systems

In the modeling performed to study O₃ non-attainment issues in North Carolina, we identified four ozone episodes that occurred during the summers of 1995, 1996 and 1997 and developed base-case applications using the MM5-SMOKE-MAQSIP modeling system. An iterative procedure was adopted to refine the base-case model performance for each episode; each time, the overall modeling system was improved by either changing the model configuration or by refining the meteorological and/or emissions inputs. Once acceptable base cases were developed per the US EPA guidance (US EPA, 1991, 1999; Russell and Dennis, 2000), we performed numerous emissions sensitivity simulations to develop future-year 2007 and 2012 attainment scenarios. We modeled a total of 16 episode days spanning the three summer periods: 12–15 July 1995, 21–24 and 27–30 June 1996 and 12–15 July

1997. These episodes were chosen based upon extensive analyses of historical episodes in North Carolina (STI, 1998); they represented typical meteorological conditions for the region, and included high 8-h ozone episodes closer to current ozone design values. For each episode, we performed simulations from 2 days prior to the actual episode start date, to provide ramp-up of the initial and boundary conditions (obtained from climatological data). The modeling domain (Fig. 1a) used

has a nested system of 36/12/4-km grids centered over North Carolina. Fig. 1b shows the zoomed-in 4-km modeling domain and the location of the air quality monitors that are the focus of this study. The various models used are described below.

2.1. Mesoscale meteorological model

The meteorological inputs for this study were derived from the Fifth-Generation Penn State/

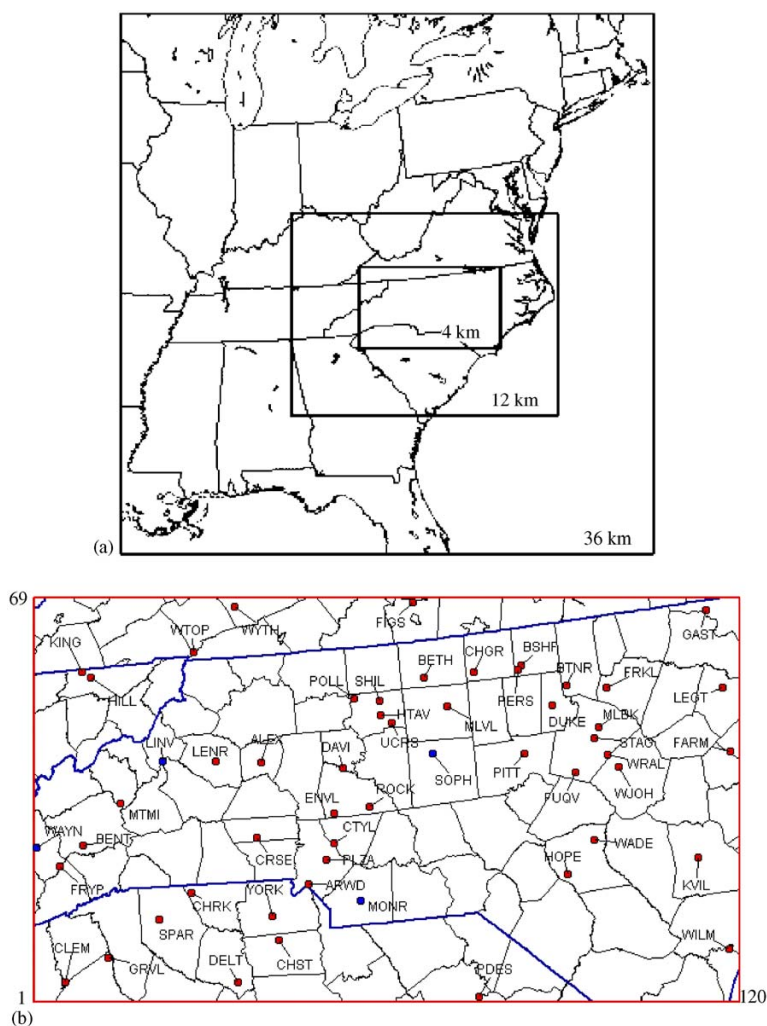


Fig. 1. (a) Nested air quality modeling domain (36-, 12- and 4-km grids) and (b) O₃ monitors in the 4-km grid (state boundaries shown in thicker/blue lines).

NCAR mesoscale model (MM5) (Grell et al., 1994). We used MM5 V1, V2.12 and V3.3 for the 1995, 1996 and 1997 episodes, respectively, since these were the latest versions that were available when we developed the base cases. We used one-way nesting in MM5, and the choices of cloud scheme and planetary boundary layer (PBL) scheme used for each grid resolution are shown in Table 1. We employed observational nudging of winds (using surface reports, profilers and soundings when available) at 12- and 4-km resolutions, and we used grid nudging at 108/36/12-km resolutions. An iterative procedure was applied to each episode to generate the best meteorological inputs possible. We changed either the PBL scheme and/or the cloud parameterization scheme during these iterations. The meteorological model performance was evaluated each time to measure improvements, by looking at the model's capability to predict key meteorological variables such as wind speed, wind direction, PBL heights, temperature and moisture (CEP, 2005).

The model was vertically resolved into 26 layers, and the top of the domain extends up to 100 mb. No interpolations were necessary from MM5 to the Multiscale Air Quality Simulation Platform (MAQSIP) model in the horizontal or vertical because the models used the same coordinate systems and grid resolutions. MAQSIP-ready meteorological inputs were derived using the meteorology-coupler (MCPL) (Coats et al., 1998). MCPL is a drop-in MM5 output module designed for coupling MM5 to other environmental models, using the Models-3 Input/Output Applications Programming Interface (Coats, 2005).

Table 1
Cloud scheme and PBL scheme used in MM5 for each episode/
grid resolution

	Episode year	36 km	12 km	4 km
Cloud Scheme	1995	Kain- Fritsch	Kain- Fritsch	Explicit
	1996	Kain- Fritsch	Kain- Fritsch	Explicit
	1997	Grell	Grell	Explicit
PBL Scheme	1995	Blackadar	Gayno- Seaman	Gayno- Seaman
	1996	Blackadar	Blackadar	Blackadar
	1997	Blackadar	Blackadar	Blackadar

2.2. Sparse matrix operator kernel emissions (SMOKE) modeling system

Emissions inputs were developed using the SMOKE (Houyoux and Vukovich, 1999; Houyoux et al., 2000) processing system. We used the beta version of SMOKE V2.0 for all emissions modeling presented here. Speciation was performed using the carbon bond mechanism-IV (CBM-IV) (Gery et al., 1989). Nonroad emissions estimates were obtained using the US EPA's NONROAD model. Biogenic emissions were processed using an implementation of the Biogenic Emissions Inventory System-3 (Vukovich and Pierce, 2002) within SMOKE. All episode-specific emissions inputs to the model for each of the four periods studied were continuously refined during development of the base-case model applications. Once acceptable model performance was established for the four episodes, we developed current-year emissions inputs (2000) and future-year emissions inputs (2007 and 2012). Emissions control strategies modeled for 2007 and 2012 include several Federal and State-specific control measures already in place or being implemented over the next few years for each state in the modeling domain. These measures will significantly reduce emissions from point, on-road mobile and nonroad mobile sources in North Carolina and neighboring states. Details of the actual emissions controls strategies modeled for the future years are discussed in NCDENR (2004). Fig. 2 shows changes in NO_x emissions in North Carolina by source category from 2000 to 2007 to 2012 for a typical episode day in 1996. Since the volatile organic compound (VOC) emissions estimates are dominated by biogenic sources and do not change much in the future years, only 2000 base-year estimates for a typical 1996 episode day are shown in Fig. 2.

2.3. Multiscale air quality simulation platform

MAQSIP (Mathur et al., 2004) is a comprehensive urban- to intercontinental-scale atmospheric chemistry-transport model, developed in collaboration with the US EPA; the model also served as a prototype for the US EPA's community multiscale air quality (CMAQ) modeling system (Dennis et al., 1996; Byun and Ching, 1999). The MM5 model is used to provide meteorological inputs to MAQSIP. In its current form, MAQSIP has been applied to study issues related to tropospheric O₃, acidic substances, and aerosol formation and pollutant

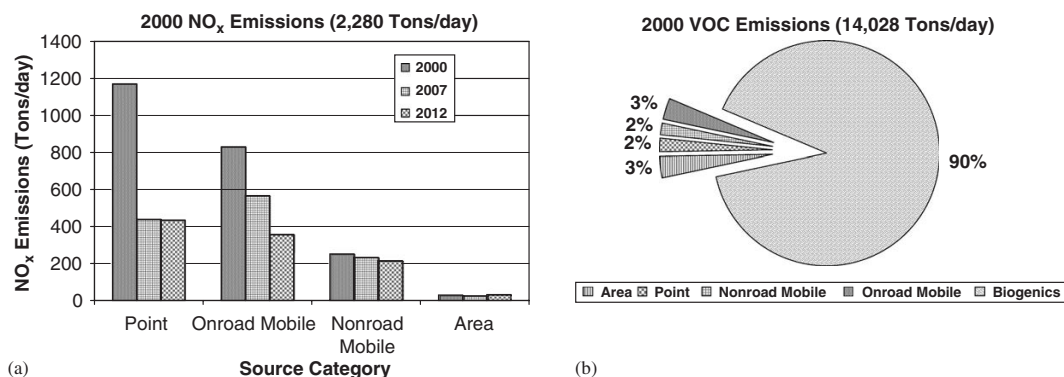


Fig. 2. NO_x (left) and VOC emissions (right) for a typical 2000 day in North Carolina.

distribution on urban, regional and intercontinental scales for various geographic areas of the world. While MAQSIP can emulate many existing atmospheric chemistry-transport models, its modular and flexible structure facilitates incorporation of new, improved process representations and algorithms. This capability allows the system to be used as a comprehensive test-bed environment for exploring different process and algorithmic representations in situ in a 3-D modeling framework with other interacting physical and chemical phenomena. Its modularity also facilitates adaptation of the model to address a broad range of atmospheric chemistry and transport problems. MAQSIP is formulated with a generalized coordinate system to better interface the chemistry-transport calculations with various meteorological models. The formulation of MAQSIP supports multiple nesting of grids for efficient resolution of smaller-scale phenomena, and allows for one-way or two-way interaction between disparate spatial scales. Thus, the model can be adapted to a variety of spatial domains ranging from urban to interregional with flexible grid resolution; simulations to date have used 4 to 108-km grid resolutions. The model also has the flexibility to use different chemical mechanisms for representing gas-phase chemistry or for incorporating explicit chemical schemes. We modeled only gas-phase chemistry for this study, and used CBM-IV with updated isoprene chemistry (Carter and Atkinson, 1996). The effects of cloud transport on the vertical distribution of trace species in the atmosphere are represented depending on the scale of model application and on the scheme used in MM5 (Mathur et al., 2004). The modular design of

MAQSIP permits a number of choices in the algorithm used for each modeled process. For this study, we modeled horizontal and vertical advection using the Bott scheme, horizontal diffusion using a constant K_h , and vertical diffusion based upon K-theory. We used one-way nesting in MAQSIP for all the episodes, and did not use plume-in-grid technique for any of the three resolutions. Several of these modules have been evaluated in detail during the course of the model development, and for subsequent other model applications; descriptions and results of the evaluations can be found separately (Kasibhatla et al., 1997; Kasibhatla and Chameides, 2000; Hogrefe et al., 2001; Fiore et al., 2003; Mathur and Dennis, 2003; Mathur et al., 1998, 2004, 2005).

2.4. Model performance evaluation

The US EPA has developed guidance documents for photochemical model performance evaluation (US EPA, 1991, 1999) that suggest specific tests and comparisons, recommend graphical methods for use in interpreting and displaying results, and identify potential issues or problems that may arise. We performed extensive evaluation of model performance for each of the episodes using observed data from the US EPA's aerometric information retrieval system (AIRS) at these sites. The list of ozone monitors is shown in Table 2. As a result of the iterative procedures adopted during the base-case development phase, we were able to achieve acceptable model performance for ozone on all 16 episode days. Fig. 3 shows daily mean normalized bias (acceptable performance is when

Table 2
O₃ monitoring sites in North Carolina and DVCs (shown in ppm)

Region	AIRS ID	ID	Site name	Site in 4 km	Ht (m)	DVCa	DVCb	Max(DVC)
Charlotte	37-119-1009	CTYL	County Line	Yes	216	0.101	0.098	0.101
	37-159-0021	ROCK	Rockwell	Yes	240	0.098	0.100	0.100
	37-159-0022	ENVL	Enochville	Yes	270	0.099	0.099	0.099
	37-119-0041	PLZA	Garinger (Plaza)	Yes	239	0.098	0.096	0.098
	37-109-0004	CRSE	Crouse	Yes	270	0.091	0.092	0.092
	37-119-1005	ARWD	Arrowood	Yes	195	0.092	0.084	0.092
	37-179-0003	MONR	Monroe	Yes	200	0.087	0.088	0.088
Triangle (Raleigh–Durham–Chapel Hill)	37-183-0014	MLBK	Millbrook	Yes	100	0.094	0.092	0.094
	37-077-0001	BTNR	Butner	Yes	91	0.092	0.094	0.094
	37-183-0015	STAG	St. Augustine	Yes	127	0.093	0.091	0.093
	37-145-0003	BSHF	Bushy Fork	Yes	198	0.089	0.091	0.091
	37-069-0001	FRKL	Franklinton	Yes	135	0.086	0.090	0.090
	37-063-0013	DUKE	Duke St.	Yes	390	0.087	0.089	0.089
	37-183-0017	WRAL	Tower	Yes	320	0.088	0.085	0.088
	37-183-0016	FUQV	Fuquay-Varina	Yes	117	0.086	0.088	0.088
	37-101-0002	WJOH	W. Johnston	Yes	127	0.087	0.085	0.087
	37-037-0004	PITT	Pittsboro	Yes	400	0.081	0.082	0.082
Triad (Greensboro–Winston–Salem–High Point)	37-059-0002	DAVI	Cooleemee	Yes	219	0.096	0.093	0.096
	37-067-0022	HTAV	Hattie Ave.	Yes	287	0.094	0.093	0.094
	37-067-1008	UCRS	Union Cross	Yes	241	0.093	0.089	0.093
	37-157-0099	BETH	Bethany	Yes	277	0.085	0.091	0.091
	37-033-0001	CHGR	Cherry Grove	Yes	285	0.090	0.088	0.090
	37-081-0011	MLVL	McLeansville	Yes	229	0.090	0.089	0.090
	37-067-0028	SHIL	Shiloh Church	Yes	294	0.089	0.088	0.089
	37-151-0004	SOPH	Sophia	Yes	250	0.085	0.085	0.085
Asheville	37-067-0027	POLL	Pollitosa	Yes	271	0.082	0.082	0.082
	37-199-0003	MTMI	Mt. Mitchell	Yes	1982	0.089	0.083	0.089
	37-087-0035	FRYP	Fry Pan	Yes	1585	0.087	0.082	0.087
	37-087-0036	PKNO	Purchase Knob	No	1494	0.087	0.085	0.087
	37-099-0005	BKNO	Barnet Knob	No	1433	0.085	0.084	0.085
	37-021-0030	BENT	Bent Creek	Yes	675	0.083	0.078	0.083
	37-087-0004	WAYN	Waynesville	Yes	802	0.080	0.079	0.080
Greenville, Rocky Mount and Wilson (Down East)	37-065-0099	LEGT	Leggett	Yes	18	0.087	0.089	0.089
	37-147-0099	FARM	Farmville	Yes	26	0.084	0.082	0.084
	37-107-0004	KINS	L. College	No	29	0.082	0.081	0.082
	37-061-0002	KVIL	Kenansville	Yes	34	0.082	0.079	0.082
	37-117-0001	JVIL	Jamesville	No	6	0.080	0.081	0.081
Fayetteville	37-051-0008	WADE	Wade	Yes	43	0.088	0.086	0.088
	37-051-1003	HOPE	Golfview	Yes	68	0.086	0.087	0.087
NW Piedmont (Hickory)	37-003-0003	ALEX	Taylorsville	Yes	339	0.087	0.088	0.088
	37-027-0003	LENR	Lenoir	Yes	366	0.087	0.084	0.087
Various areas	37-131-0002	GAST	Gaston	Yes	40	0.082	0.084	0.084
	37-029-0099	CAMD	Camden	No	3	0.080	0.081	0.081
	37-011-0002	LINV	Linville	Yes	987	0.078	0.078	0.078
	37-129-0002	WILM	Castle Hayne	Yes	12	0.075	0.078	0.078
CASTNET Sites	37-123-8001	CAND	Candor	Yes	n/a	0.086	n/a	0.086
	37-011-8001	CRAN	Cranberry	Yes	1219	0.083	n/a	0.083
	37-113-8001	COWE	Coweeta	No	686	0.077	n/a	0.077
	37-031-8001	BEAU	Beaufort	No	n/a	0.076	n/a	0.076

Note: DVCs > 0.084 ppm are shown in bold font.

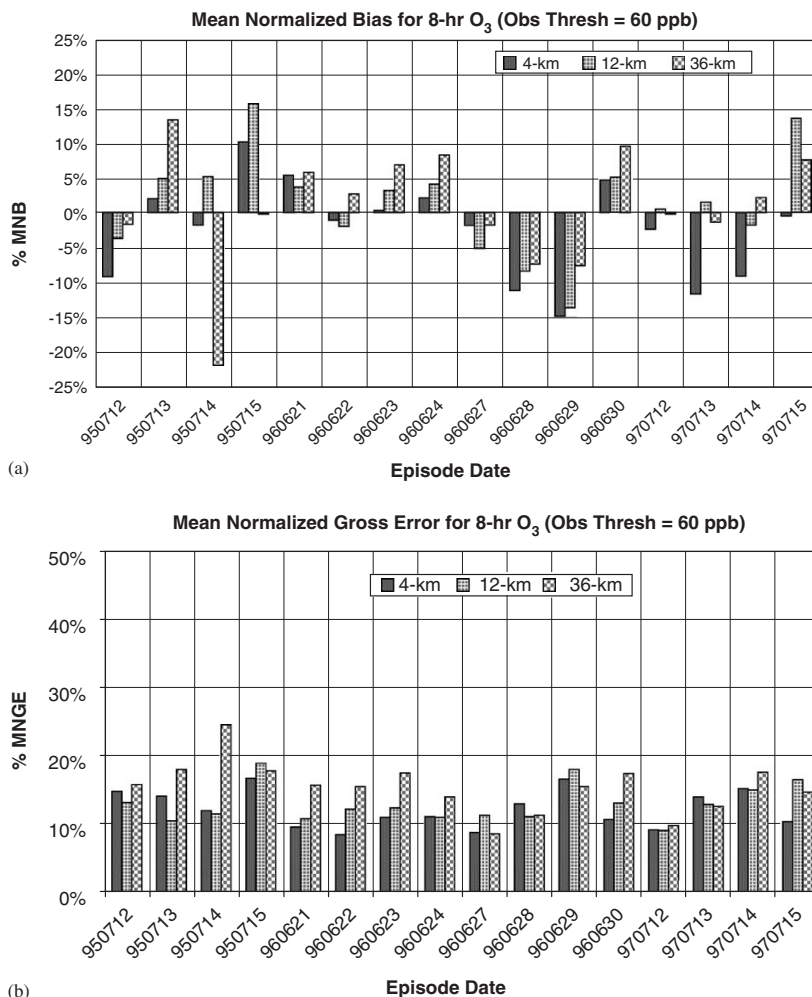


Fig. 3. Mean normalized bias and mean normalized gross error for 8-h O₃ using an observed threshold of 60 ppb.

MNB < $\pm 15\%$) and mean normalized gross error (acceptable performance is when MNGE < 35%) (Russell and Dennis, 2000) for 8-h O₃ computed at North Carolina sites in each of the three model grid resolutions. These metrics correspond to the final base-case modeling that used episode-specific emissions. In computing these metrics, we used all hourly 8-h ozone modeled predictions that corresponded to an observed threshold of 0.060 ppm. Traditionally, for attainment demonstration purposes, the focus has been on using this threshold to evaluate the model's capability to predict values that are closer to the NAAQS (US EPA, 1991), and to help reduce apparent model errors (due to

overpredictions of very low observations). However, we also computed MNB and MNGE for 8-h ozone using an observed threshold of 0.005 ppm (shown in Fig. 4), and one can see the relatively large bias and large errors when using low concentrations. Additional results from model performance evaluation performed for these episodes are also available (Arunachalam et al., 2001, 2002; CEP, 2005; NCDENR, 2004).

3. Attainment demonstration

This paper focuses on an evaluation of the MM5-SMOKE-MAQSIP modeling system for

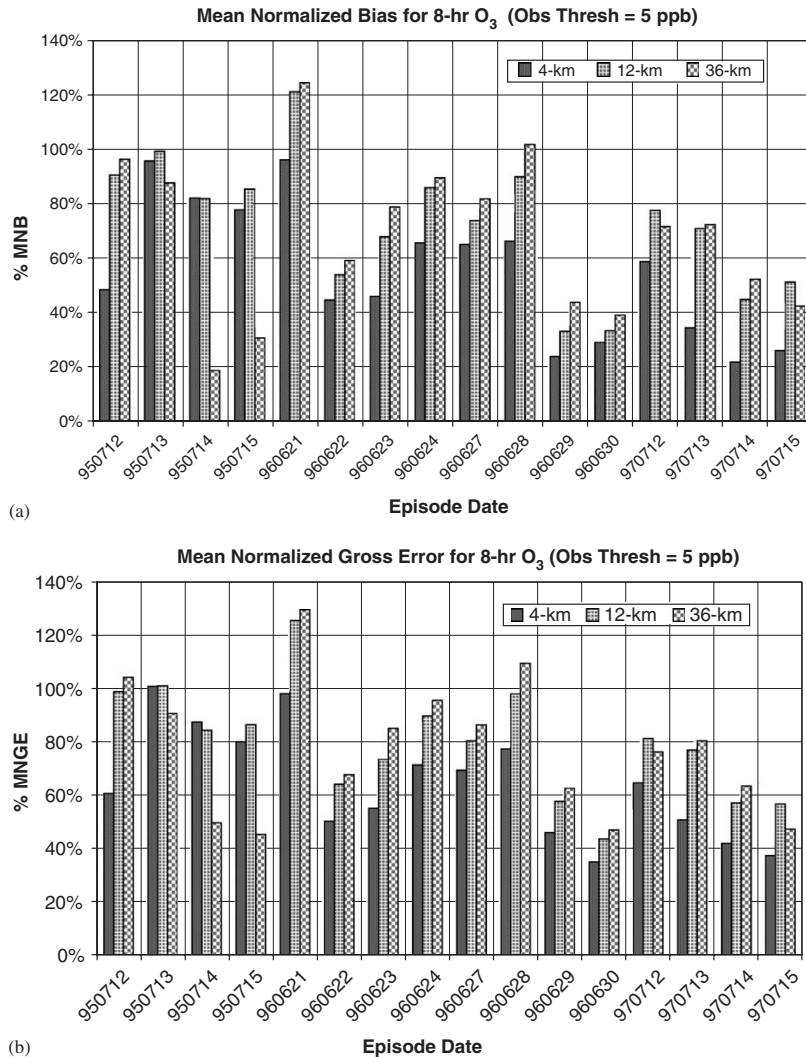


Fig. 4. Mean normalized bias and mean normalized gross error for 8-h O₃ using an observed threshold of 5 ppb.

predicting future-year air quality using a demonstration of the US EPA's modeled attainment test (US EPA, 1999) in the North Carolina modeling domain (Fig. 1a and b). The attainment test to determine whether a given monitor meets the NAAQS or not by the mandated future year, recommends using modeled predictions in a relative sense rather than an absolute sense. A key assumption underlying the use of the relative reduction factor (RRF) in demonstrating attainment is that the uncertainty in the difference

between the ozone maximum predictions for the base and emissions control scenarios is less than the uncertainty in the ozone maximum predictions themselves (Hanna et al., 2001). Further, this attainment test is closely tied to the form of the NAAQS for 8-h ozone.

3.1. Modeled attainment test

For this study, we applied the modeled attainment test only to North Carolina O₃ monitors in the

4-km grid (see Fig. 1b). The site-specific future-year air quality is computed as follows:

1. Calculate the site-specific current design values (DVCs) from monitored data.

To be consistent with the form of the NAAQS, we calculated the DVC at each site by using the fourth-highest daily maximum 8-h O_3 concentration in each of three consecutive years (chosen as discussed next), and then finding their arithmetic mean. Because there is likely to be some variability in observed design values due to meteorological variations, the higher of the following two values was chosen: (a) average design value from the 3-year period “straddling” the year represented by the most recent available emissions inventory (1999–2001), indicated by DVCa in Table 2; and (b) average design value from the 3-year period (2001–2003) used to designate an area “nonattainment”, shown as DVCb in Table 2. Using the maximum of these two values ensures that DVCs are not underestimated.

Table 2 lists the monitors in North Carolina grouped by urban area, along with various site characteristics, including the DVC for each site. From Table 2 and from Fig. 1b, one can see that there is a very extensive monitoring network in North Carolina, and in some instances, the monitors are located very close to each other (within a few kilometers).

2. Use air quality modeling results to estimate site-specific RRFs.

In this step, we identified surface grid cells that were considered to be “near” a monitoring site, rather than just the cell containing the monitor. Since it is hypothesized that RRFs can be underestimated due to potential migration of the predicted O_3 peak that results from a chosen control strategy, we identified a 15-km radius as being “near” a site, i.e., as an area consistent with the intended representativeness for urban-scale O_3 monitors (US EPA, 1999). The size of the array of “nearby” cells around each site varied for each grid resolution. For the 36-km resolution, it was a 1×1 array; for the 12 km, a 3×3 array; and for the 4 km, a 7×7 array. The spatial extents of these grid-cell clusters are shown in Fig. 5 using a typical episode day’s daily maximum 8-h O_3 predictions in the base-year, i.e., for 22 June 2000. This figure also shows the spatial variability of the daily maximum

values within the “nearby” cells at each site for each of the three grid resolutions. It can be hypothesized that the monitor is at the center of the cell in which it is located, and that this cell is at the center of the appropriate array (e.g., at the center of a 7×7 array of “nearby” cells in the case of the 4-km grid). The elevation of the monitor is not a factor while defining the “nearby” cells.

We computed the site-specific RRFs for each grid resolution as follows:

- (a) Compute the daily maximum 8-h O_3 concentration in every grid cell for each modeled episode day in the base case. (After establishing model performance for the base case with episodic emissions inputs, MAQSIP was run using the “current-year” emissions [i.e., 2000] for use in the base-year calculations.)
 - (b) From these values, find each day’s highest predicted daily maximum 8-h O_3 concentration.
 - (c) Compute the average of the highest values for all modeled episode days, using only those days when the highest was ≥ 0.070 ppm, to get a site-specific mean base-year value (Mean_BY). The threshold of 0.070 ppm is applied to exclude low-value days that would cause overestimation of future-year design values (calculated in step 3 below). In some instances, this led to using fewer than 16 episode days in computing Mean_BY.
 - (d) Repeat steps (a)–(c) for the future-year projected case, using the same days to average in the future-year calculation as were used in the base-year calculation, to get a site-specific mean future-year value (Mean_FY). Note that on any given day, the grid cell chosen for the future-year case need not be the same as the one chosen in the base-year case, and this helps to capture the ‘migration’ of a predicted peak from the base-year to the future-year case.
 - (e) Calculate the relative reduction factor: $RRF = \text{Mean_FY} / \text{Mean_BY}$.
3. Compute site-specific future-year design values (DVF): $DVF = DVC \times RRF$.
 4. Compare all DVFs to NAAQS for 8-h O_3 .
If all the calculated DVFs are ≤ 0.084 ppm, the modeled attainment test has been passed, and the modeling domain is set to be in attainment of the US NAAQS for 8-h O_3 in the modeled future year. Although the level of the 8-h O_3 NAAQS is

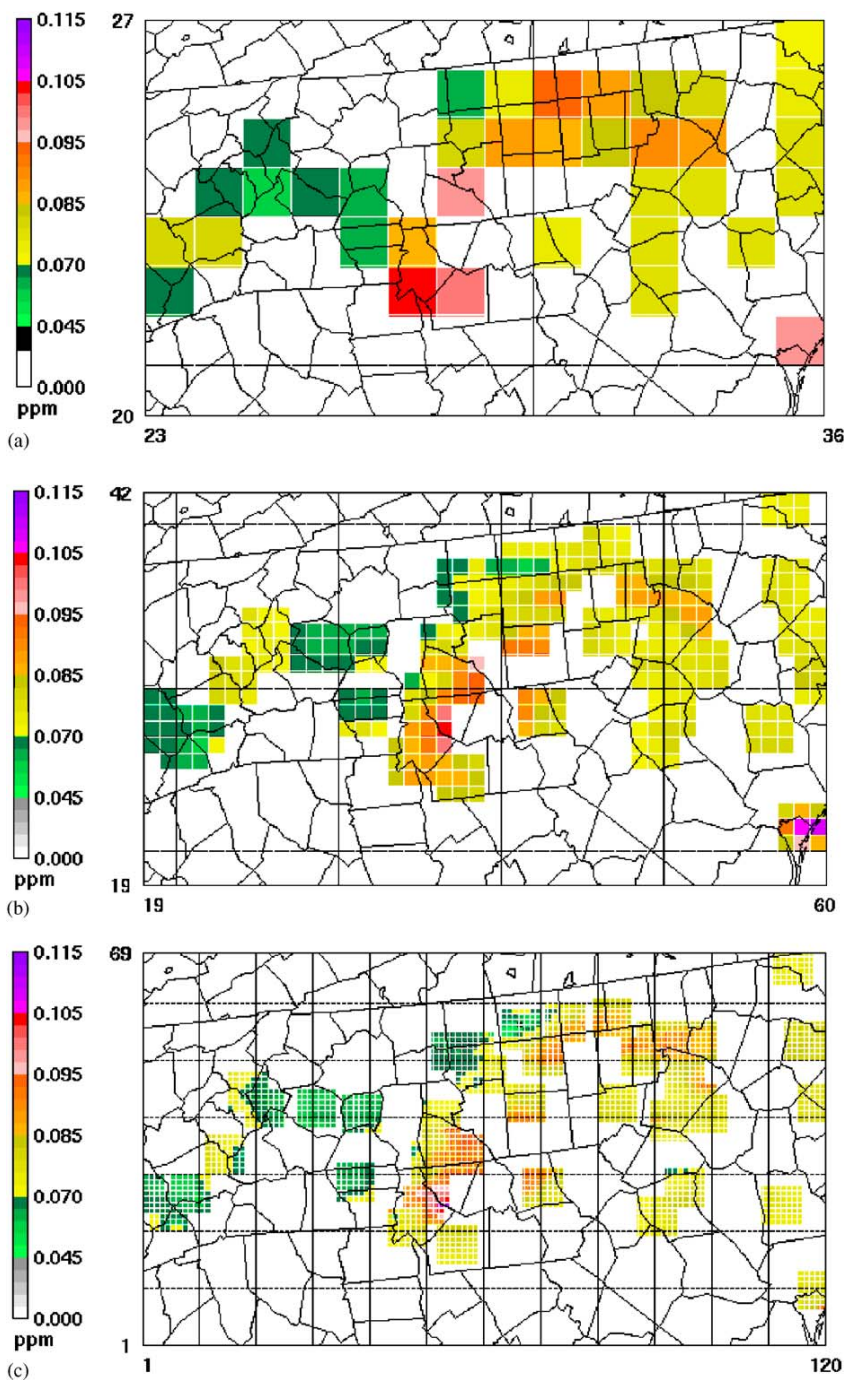


Fig. 5. “Nearby” grid cells around the monitors in 36- (top), 12- (middle) and 4-km (bottom) grid resolutions shown for a typical base-year day’s daily maximum 8-h O_3 in 2000.

0.080 ppm, the third decimal digit, in ppm, is rounded. Hence, 0.084 ppm is the largest concentration that is ≤ 0.080 ppm.

4. Results and discussion

Using each episode's meteorology, we performed current-year (2000) and future-year simulations for 2007 and 2012. We then postprocessed the model results as discussed above to compute Mean_BY and Mean_FY values (from the 16 episode days) and then finally the RRFs and DVFs for each of 2007 and 2012. Table 3 shows the 2007 and 2012 DVFs for all North Carolina ozone monitors.

Fig. 6 (left column) shows the variation of DVFs and 2007 RRFs and DVFs vs. Mean_BY O_3 computed using model outputs from each of the 36-, 12- and 4-km grid resolutions. All North Carolina monitors in each of these grid resolutions are shown in these plots, and one should note that the 4-km domain consisted of less number of monitors than the other domains. Hence, the 36- and 12-km plots show more data points than the 4-km plot. A 0.085 ppm line is also shown as the level of the 8-h O_3 NAAQS exceedance. When we use the 36-km computed RRFs, only two sites—County Line (DVF of 0.086 ppm) and Enochville (0.085 ppm) in the Charlotte region—are still shown to be in nonattainment. Using the 12-km computed RRFs, four sites—County Line (0.087 ppm), Rockville (0.087 ppm), Enochville (0.086 ppm) and Plaza (0.085 ppm) in the Charlotte region—are shown to be in nonattainment. The 4-km computed RRFs yield an identical DVF of 0.087 ppm at all of these four sites. Similar metrics for the 2012 future-year scenario (Fig. 6, right column) indicate that all sites are in attainment of the 8-h O_3 NAAQS using RRFs from each of the three grid resolutions. As in 2007, the 2012 DVFs are also mostly similar between the 12- and 4-km resolutions, but show slightly larger differences between the 36- and 4-km modeled outputs. Interestingly, for both 2007 and 2012, the four Charlotte-region sites just referenced have higher base-year ozone concentrations with the 12-km grid than with the 36- or 4-km grids. Note that although the circles representing DVFs (a y-axis variable) change location as the grid-resolution changes, it is actually the change in Mean_BY values (x-axis) that cause the DVC circles to move. The DVFs themselves remain constant across all grid resolutions.

To facilitate comparisons, the variations of the 36-, 12- and 4-km 2007 and 2012 RRFs vs. the corresponding DVFs are shown on the same plot in Fig. 7, while Fig. 8 shows similar plots of DVFs vs. DVFs. These plots illustrate the almost identical response of the modeling system in the 12 km when compared to the 4 km. This seems to indicate that the artificial dilution of emissions within coarse-grid resolutions plays a relatively bigger impact in predicting model responses at 36 km than at 12-km grid resolution. Thus, the underlying combination of physical and chemical processes that contribute to ozone exceedances and their reductions is similar in the 12- and 4-km grid resolutions, but not at 36 km. Table 4 gives the number of monitors that show differences in RRFs when comparing 4-km model outputs to 12- or 36-km outputs. For 2007, the RRFs computed using 4-km outputs at 38 out of 42 sites have either 0% or $<3\%$ difference compared to the 12-km outputs. Not a single site shows a difference of $>5\%$. However, comparing the 4-km RRFs to the 36-km RRFs, only 26 sites have either 0% or $<3\%$ differences, and six sites have differences of $>5\%$. These differences in RRFs translate to DVF differences on the order of 1–3 ppb at most of these sites. These results corroborate the findings by Jones et al. (2005) where they showed that modeled DVFs can have uncertainties of about 2–4 ppb just through differences in alternate options to modeling.

For the 2012 4-km RRFs, 37 and 21 sites have differences of $<3\%$ when compared to the 12- and 36-km RRFs, respectively. Only one site (Fry Pan in the Asheville high-elevation region) shows $>5\%$ difference for the 2012 4-km RRF vs. 12-km RRF.

Interestingly, all six sites (Bushy Fork, Pittsboro, Cherry Grove, Bent Creek, Waynesville and Castle Hayne) that have $>5\%$ difference in 2007 RRFs (4 vs. 36 km) show $>5\%$ differences in the 2012 RRFs (4 vs. 36 km) too. Also, all four sites (Pittsboro, Fry Pan, Bent Creek and Waynesville) that show differences of $>3\%$ in 2007 RRFs (4 vs. 12 km) also have differences of $>3\%$ in 2012 RRFs (4 vs. 12 km), with Fry Pan showing a notable increase from -3.4% (in 2007) to -7.1% (in 2012) difference in RRF.

4.1. Statistical significance

To further quantify the differences (or similarities) between the model responses in different grid resolutions, we used the Student's *t*-test (Steel et al., 1997) for the second part of the analyses. As we

Table 3
O₃ design values and *p*-values from Student's *t*-tests

Region	ID	DVC	2007 DVF			2012 DVF			<i>p</i> -Value (12 vs. 4)	
			36 km	12 km	4 km	36 km	12 km	4 km	2007	2012
Charlotte	CTYL	0.101	0.086	0.087	0.087	0.079	0.080	0.081	0.79	0.57
	ROCK	0.100	0.084	0.087	0.087	0.077	0.080	0.080	0.75	0.90
	ENVL	0.099	0.085	0.086	0.087	0.078	0.080	0.081	0.39	0.47
	PLZA	0.098	0.084	0.085	0.087	0.077	0.080	0.080	0.82	0.85
	CRSE	0.092	0.078	0.079	0.080	0.072	0.074	0.076	0.56	0.38
	ARWD	0.092	0.079	0.082	0.082	0.073	0.077	0.078	0.77	0.79
	MONR	0.088	0.074	0.077	0.075	0.070	0.071	0.070	0.10	0.24
Triangle (Raleigh–Durham–Chapel Hill)	MLBK	0.094	0.080	0.080	0.080	0.074	0.073	0.075	0.85	0.76
	BTNR	0.094	0.078	0.079	0.079	0.072	0.075	0.074	0.57	0.78
	STAG	0.093	0.079	0.080	0.080	0.073	0.074	0.074	0.87	0.84
	BSHF	0.091	0.070	0.077	0.077	0.066	0.073	0.072	0.45	0.47
	FKL	0.090	0.077	0.077	0.078	0.071	0.071	0.072	0.70	0.54
	DUKE	0.089	0.076	0.077	0.075	0.070	0.070	0.070	0.76	0.97
	WRAL	0.088	0.075	0.076	0.075	0.068	0.070	0.068	0.50	0.65
	FUQV	0.088	0.075	0.073	0.075	0.070	0.068	0.070	0.54	0.46
	WJOH	0.087	0.074	0.075	0.074	0.068	0.068	0.068	0.83	0.97
	PITT	0.082	0.067	0.068	0.071	0.060	0.063	0.065	0.15	0.04
Triad (Greensboro–Winston Salem–High Point)	DAVI	0.096	0.080	0.083	0.084	0.073	0.076	0.079	0.36	0.20
	HTAV	0.094	0.078	0.079	0.080	0.073	0.074	0.075	0.93	0.82
	UCRS	0.093	0.078	0.079	0.079	0.071	0.073	0.073	0.92	1.00
	BETH	0.091	0.076	0.076	0.076	0.071	0.073	0.071	0.72	0.79
	CHGR	0.090	0.070	0.074	0.076	0.064	0.071	0.072	0.68	0.57
	MLVL	0.090	0.075	0.077	0.076	0.068	0.071	0.071	1.00	0.93
	SHIL	0.089	0.073	0.078	0.076	0.068	0.072	0.072	0.26	0.49
	SOPH	0.085	0.071	0.072	0.072	0.065	0.066	0.067	0.97	0.75
	POLL	0.082	0.068	0.069	0.069	0.063	0.064	0.065	0.78	0.62
Asheville	MTMI	0.089	0.072	0.074	0.075	0.067	0.070	0.071	0.58	0.58
	FRYP	0.087	0.073	0.074	0.077	0.069	0.068	0.073	0.03	0.02
	PKNO	0.087	0.073	0.075	n/a	0.066	0.070	n/a	n/a	n/a
	BKNO	0.085	0.070	0.073	n/a	0.066	0.068	n/a	n/a	n/a
	BENT	0.083	0.068	0.071	0.074	0.063	0.067	0.069	0.02	0.03
	WAYN	0.080	0.067	0.068	0.071	0.060	0.064	0.067	0.20	0.10
Greenville, Rocky Mount and Wilson (Down East)	LEGT	0.089	0.080	0.076	0.077	0.074	0.070	0.072	0.59	0.38
	FARM	0.084	0.073	0.074	0.073	0.069	0.070	0.068	0.62	0.77
	KINS	0.082	0.072	0.073	n/a	0.068	0.069	n/a	n/a	n/a
	KVIL	0.082	0.071	0.072	0.072	0.066	0.067	0.068	0.83	0.94
	JVIL	0.081	0.073	0.073	n/a	0.070	0.070	n/a	n/a	n/a
Fayetteville	WADE	0.088	0.077	0.077	0.078	0.070	0.071	0.073	0.90	0.70
	HOPE	0.087	0.077	0.077	0.077	0.070	0.071	0.072	0.84	0.53
NW Piedmont (Hickory)	ALEX	0.088	0.074	0.075	0.075	0.069	0.069	0.069	0.62	0.81
	LENR	0.087	0.073	0.074	0.073	0.068	0.069	0.068	0.91	0.73
Various areas	GAST	0.084	0.073	0.073	0.073	0.069	0.069	0.069	0.95	0.76
	CAMD	0.081	0.073	0.076	n/a	0.071	0.074	n/a	n/a	n/a
	LINV	0.078	0.065	0.066	0.067	0.060	0.061	0.063	0.94	0.75
	WILM	0.078	0.065	0.069	0.069	0.062	0.065	0.066	0.70	0.93
CASTNET Sites	CAND	0.086	0.074	0.073	0.073	0.069	0.068	0.068	0.39	0.61
	CRAN	0.083	0.068	0.069	0.070	0.063	0.065	0.066	0.77	0.99
	COWE	0.077	0.066	0.066	n/a	0.062	0.060	n/a	n/a	n/a
	BEAU	0.076	0.066	0.067	n/a	0.063	0.064	n/a	n/a	n/a

Note: Design values > 0.084 ppm are shown in bold font.

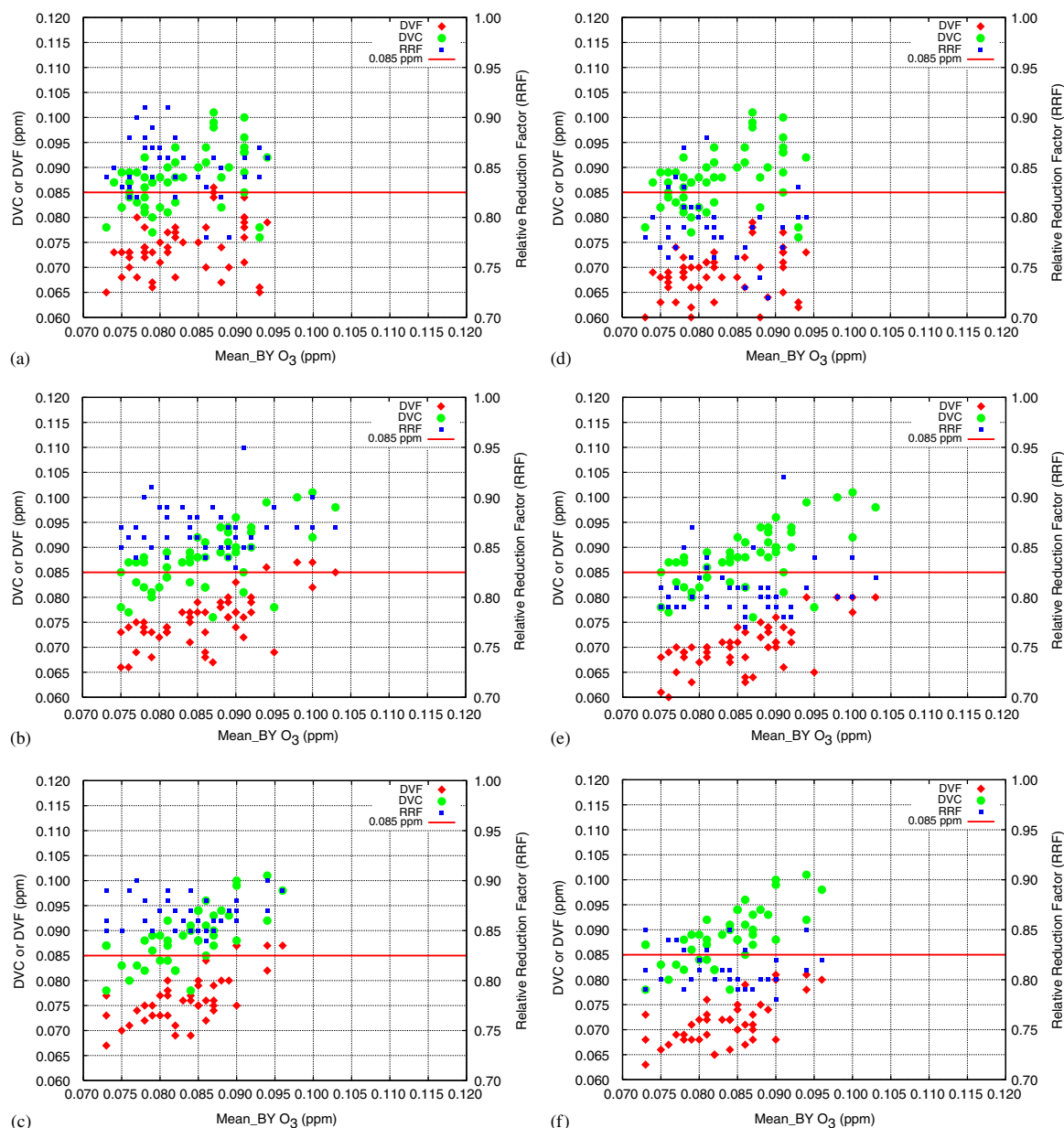


Fig. 6. Mean base-year O₃ vs. DVCs, RRFs and DVFs from 36- (top), 12- (middle) and 4-km (bottom) grid resolutions, shown for 2007 (left column) and 2012 (right column).

discussed earlier, the only factor that changes DVFs (between future years or between grid resolutions) is the RRFs. Since DVCs remain constant for all grid resolutions, for the Student's *t*-test it was appropriate to focus on RRFs, the key determinant for attainment. The test was to determine whether the daily RRFs for the 12-km grid are equal to

the daily RRFs for the 4-km grid, for each monitoring site. The null hypothesis was defined as no difference between the mean daily RRFs from the 12-km grid and the 4-km grid, i.e., $H_0: \mu_{12} - \mu_4 = 0$ (or $\mu_{12} = \mu_4$) and $H_1: \mu_{12} - \mu_4 \neq 0$ (or $\mu_{12} \neq \mu_4$). Assuming that the two populations from which the samples were drawn have unequal

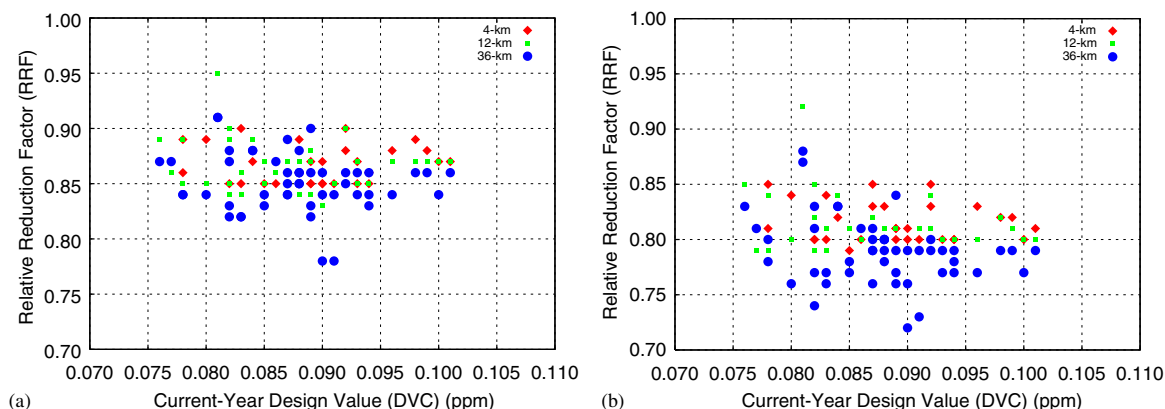


Fig. 7. Variation of DVCs vs. 2007 RRFs (left) and 2012 RRFs (right).

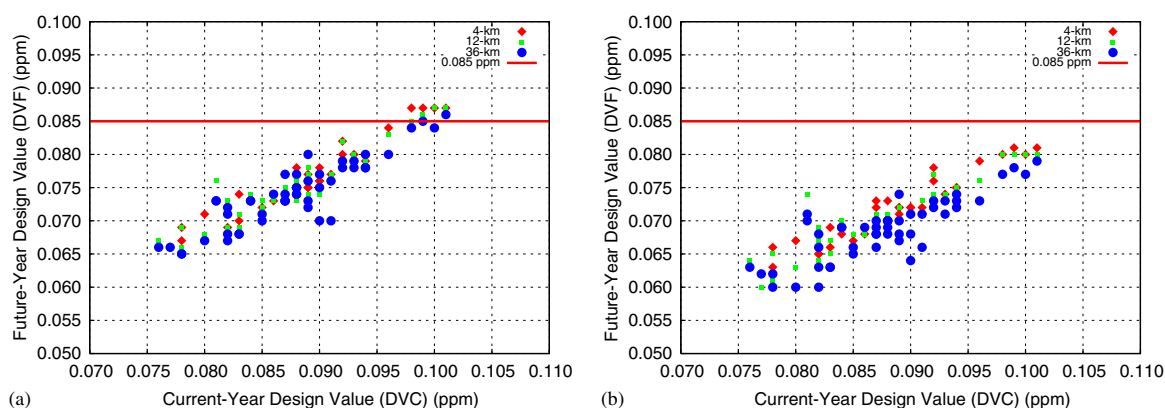


Fig. 8. Variation of DVCs vs. 2007 DVF (left) and 2012 DVF (right).

Table 4

Number of sites that have differences in 12- and 36-km RRFs compared to 4 km

Magnitude of RRF differences (%)	2007 4 vs. 12 km	2007 4 vs. 36 km	2012 4 vs. 12 km	2012 4 vs. 36 km
0	15	7	11	9
<3	23	19	26	12
3–5	4	10	4	12
>5	0	6	1	9

variances ($\sigma_{12}^2 \neq \sigma_4^2$), the appropriate variance for use in calculating t -statistics is computed as

$$s_{(\bar{Y}_{12} - \bar{Y}_4)} = \sqrt{\frac{(s_{12})^2}{n_{12}} + \frac{(s_4)^2}{n_4}},$$

where n_{12} and n_4 are the number of episode days used in calculating the mean daily RRFs for the 12- and 4-km grids, and hence had a maximum value of 16, $(s_{12})^2$ and $(s_4)^2$ are the sample variances for the 12- and 4-km grids, and \bar{Y}_{12} and \bar{Y}_4 are the monitor-specific mean daily RRFs for the 12- and

4-km grids. The corresponding t -statistic is then defined as

$$t' = \frac{\bar{Y}_{12} - \bar{Y}_4}{s_{\bar{Y}_{12} - \bar{Y}_4}}$$

with an effective degree of freedom equal to

$$df = \frac{(s_{12}^2/n_{12}) + (s_4^2/n_4)}{[(s_{12}^2/n_{12})/(n_{12} - 1)] + [(s_4^2/n_4)/(n_4 - 1)]}$$

One should note that the t -statistic presented in the paper is t' . The prime indicates that, due to the test setup, the t -statistic is not distributed strictly as a Student's t but as an approximation to it. The approximate nature dictates that we use an effective degree of freedom with the tabulated t as opposed to a more common calculation of the degrees of freedom.

Table 3 also shows the results of the t -test by presenting the p -values for each monitor, when comparing the RRFs from the 12 and 4 km for each of the two future years. Using a significance level of $\alpha = 0.05$, any p -value < 0.05 would be significant, and the null hypothesis is rejected in favor of the alternative hypothesis. A low p -value for the statistical test indicates rejection of the null hypothesis because it indicates how unlikely it is that a test statistic as extreme as, or more extreme than the one given by these data will be observed from this population if the null hypothesis is true. For example, if $p = 0.012$, this means that if the population means were equal as hypothesized (under the null), there is a 12 in 1000 chance that a more extreme test statistic would be obtained using data from this population. If one agrees that there is enough evidence to reject the null hypothesis, one may conclude that there is significant evidence to support the alternative hypothesis. Applying the Student's t -test on a per-monitor basis helps isolate areas (or monitors) that may benefit from the finer grid resolution.

Of all the North Carolina sites analyzed, Bent Creek and Fry Pan accept H_1 , i.e., the 12- and 4-km RRFs are different for both 2007 and 2012 future-year emissions scenarios. Pittsboro rejected H_0 only for 2012. For all the other sites in North Carolina, the differences between the RRFs from the 12 and 4 km were statistically insignificant. Additional examination of the sites that reject H_0 reveal that all three sites have DVCs which are near attainment (≤ 0.087 ppm), and DVFs well below the NAAQS (≤ 0.077 ppm). Both Bent Creek and Fry Pan are

situated at high elevations, and we believe that topography at these sites may contribute to significant differences in RRFs between the two grid resolutions; at these locations, the models are blending air masses of different origins and the 12-km grid artificially dilutes NO_x emissions over a relatively larger grid volume. Pittsboro is a special case since it is a rural site that lies at the edge of the Triangle urban area, and may also be affected by a major NO_x source (Cape Fear power plant) in its vicinity. Given these two reasons, the emissions gradient and hence the individual values in the daily maxima array in the 'nearby' cells in each of the 4- and 12-km grids may undergo a rapid transition and hence contribute to different RRFs. Furthermore, the effect of NO_x titration from the Cape Fear source may also lead to differences in the RRFs between the two grid resolutions.

The US EPA draft guidance for demonstrating attainment of the NAAQS for $\text{PM}_{2.5}$ nonattainment areas (US EPA, 2001) recommends a similar approach for computing RRFs and then DVFs for future years. For urban areas, the US EPA recommends that states use a 12-km grid resolution for estimating RRFs for secondary particulate matter, but a much finer resolution of 5 km or less for primary particulate matter. Since there is an annual standard for $\text{PM}_{2.5}$, states may resort to performing annual base-year and future-year simulations to compute RRFs and DVFs; this will impose a huge burden on computational resources, especially for fine-grid modeling of longer periods. Based upon our application of the draft guidance for O_3 attainment purposes, we recommend that similar model evaluation be performed for $\text{PM}_{2.5}$ nonattainment areas to obtain ranges of variability for future-year $\text{PM}_{2.5}$ concentrations at various grid resolutions. States could then consider the use of coarse-grid resolutions, say 12 km for annual modeling to compute RRFs and DVFs for primary particulate matter as well, and then use the information gained from benchmark studies like these as bounds of variability to supplement the modeling results.

5. Conclusions

We used the MM5-SMOKE-MAQSIP modeling system to study future-year attainment of the 8-h O_3 NAAQS in several urban areas of North Carolina using a diverse set of meteorological (four different episodes in 1995, 1996 and 1997), chemical (two

different future-year emissions scenarios—2007 and 2012) and physical (in three different model grid resolutions—36, 12 and 4 km) conditions. Using extensive model performance evaluation, we first established that the modeling systems performed well in capturing historical O₃ exceedances before using them in a relative sense for the future years.

Using an illustration of the US EPA's guidance for 8-h O₃ attainment demonstration in North Carolina, the results (focused on predicted RRFs and DVFs) show the potential uncertainty in modeled results due to grid resolution. Specifically, out of 42 sites analyzed in North Carolina, 38 (in the case of 2007) and 37 (in the case of 2012) sites have 12-km RRFs that differ by only <3% when compared to the 4-km RRFs. However, only 26 (in the case of 2007) and 21 (in the case of 2012) sites show <3% differences in the 36-km RRFs vs. 4-km RRFs, which indicates the sensitivity of the RRFs to the grid resolution modeled. In general, the coarser the grid resolution, the greater is the model response, and hence slightly lower are the RRFs. We were able to quantify the grid-resolution variability using the Student's *t*-test, which showed that the differences between the 4- and 12-km computed RRFs were statistically insignificant except for three sites. These differences in RRFs (between the 36- and 4-km predictions) translate to an average difference of 1–3 ppb in the DVFs for some sites, and we recommend that this estimate of 1–3 ppb be considered as the estimate of variability due to grid resolution in the modeling. Based upon these results, future attainment demonstration studies (for ozone and perhaps PM_{2.5}) may consider using RRFs and DVFs from 12-km modeling and incorporate variability estimates into them.

Acknowledgments

The authors would like to thank the Division of Air Quality (DAQ) under the North Carolina Department of Environment and Natural Resources for funding this work, under Modeling Assistance Contracts EA2012, EA03017 and EA05009. We also gratefully acknowledge Donald Olerud of Baron Advanced Meteorological Systems for the meteorological modeling and evaluation, the emissions modeling staff at DAQ for preparing the emissions inputs, Zac Adelman, Jeff Vukovich and Kim Hanisak of the Carolina Environmental Program for their assistance with preparing various other inputs, and George Bridgers of the DAQ for

his contributions throughout this project. We also thank Jeanne Eichinger for her assistance with editing the final version of the manuscript. We finally thank the two anonymous reviewers for their valuable comments and suggestions that helped improve the overall quality of this paper.

References

- Arunachalam, S., Adelman, Z., Mathur, R., Olerud, D., Holland, A., 2001. A comparison of the Models-3/CMAQ and MAQSIP modeling systems for O₃ modeling in North Carolina. In: Proceedings of the 94th Annual Meeting of the Air and Waste Management Association, 25–28 June 2001, Orlando, FL.
- Arunachalam, S., Adelman, Z., Mathur, R., Vukovich, J., 2002. The impacts of biogenic emissions estimates from BEIS-3 on ozone modeling in the southeastern US. In: Proceedings of the 11th Annual Emissions Inventory Conference: Emissions Inventories—Partnering for the Future. US Environmental Protection Agency, 15–18 April 2002, Atlanta, GA.
- Byun, D.W., Ching, J.K.S. (Eds.), 1999. Science Algorithms of the EPA Models-3 Community Multiscale Air Quality (CMAQ) Modeling System. EPA/600/R-99/030. US Environmental Protection Agency, Research Triangle Park, NC.
- Carter, W.P.L., Atkinson, R., 1996. Development and evaluation of a detailed mechanism for the atmospheric reactions of isoprene and NO_x. *International Journal of Chemical Kinetics* 28, 497–530.
- Carolina Environmental Program (CEP), 2005. NCDAQ 8-h O₃ modeling project web site. <<http://www.cep.unc.edu/empdp/projects2/NCDAQ/PGM/results>> (accessed October 2005).
- Coats, C.J., 2005. The EDSS/Models-3 I/O Applications Programming Interface web site. <<http://www.baronams.com/products/ioapi>> (accessed October 2005).
- Coats, C.J., McHenry, J., Lario-Gibbs, A., Peters-Lidard, C., 1998. MCPL: a drop-in MM5 module suitable for coupling MM5 to parallel environmental models. Eighth PSU/NCAR Mesoscale Model User's Workshop, 15–16 June 1998, Boulder, CO, pp. 117–120.
- Dennis, R.L., Byun, D.W., Novak, J.H., Galluppi, K.J., Coats, C.J., 1996. The next generation of integrated air quality modeling: EPA's Models-3. *Atmospheric Environment* 30, 1925–1938.
- Federal Register, 18 July 1997. 62 FR 38856.
- Federal Register, 30 April 2004. 69 FR 23857.
- Fiore, A.M., Jacob, D.J., Mathur, R., Martin, R.V., 2003. Application of empirical orthogonal functions to evaluate ozone simulations with regional and global models. *Journal of Geophysical Research* 108 (D14), 4431.
- Gery, M.W., Whitten, G.Z., Killus, J.P., Dodge, M.C., 1989. A photochemical kinetics mechanism for urban and regional scale computer modeling. *Journal of Geophysical Research* 94 (D10), 12,925–12,956.
- Grell, G.A., Dudhia, J., Stauffer, D.R., 1994. A Description of the Fifth-Generation Penn State/NCAR mesoscale model (MM5). NCAR Technical Note TN-398. National Center for Atmospheric Research, Boulder, CO.
- Hanna, S.R., et al., 2001. Uncertainties in predicted ozone concentrations due to input uncertainties for the UAM-V

- photochemical grid model applied to the July 1995 OTAG domain. *Atmospheric Environment* 35 (5), 891–903.
- Hogrefe, C., Rao, S.T., Kasibhatla, P., Hao, W., Sistla, G., Mathur, R., McHenry, J., 2001. Evaluating the performance of regional-scale photochemical modeling systems: Part II. O₃ predictions. *Atmospheric Environment* 35 (24), 4175–4188.
- Houyoux, M.R., Vukovich, J.M., 1999. Updates to the SMOKE modeling system and integration with Models-3. In: *Proceedings of the Emission Inventory: Regional Strategies for the Future*. Air and Waste Management Association, 26–28 October 1999, Raleigh, NC.
- Houyoux, M.R., Vukovich, J.M., Coats Jr., C.J., Wheeler, N.J.M., Kasibhatla, P.S., 2000. Emission inventory development and processing for the Seasonal Model for Regional Air Quality (SMRAQ) project. *Journal of Geophysical Research* 105 (D7), 9079–9090.
- Jang, J.-C.C., Jeffries, H.E., Byun, D., Pleim, J.E., 1995a. Sensitivity of ozone to model grid resolution: I. Application of high-resolution regional acid deposition model. *Atmospheric Environment* 29 (21), 3085–3100.
- Jang, J.-C.C., Jeffries, H.E., Tonnesen, S., 1995b. Sensitivity of ozone to model grid resolution: II. Detailed process analysis for ozone chemistry. *Atmospheric Environment* 29 (21), 3101–3114.
- Jones, J.M., Hogrefe, C., Henry, R.F., Ku, J.-Y., Sistla, G., 2005. An assessment of the sensitivity and reliability of the relative reduction factor approach in the development of 8-h ozone attainment plans. *Journal of the Air and Waste Management Association* 55, 13–19.
- Kasibhatla, P., Chameides, W.L., 2000. Seasonal modeling of regional O₃ pollution in the eastern US. *Geophysical Research Letters* 27 (9), 1415–1418.
- Kasibhatla, P., Chameides, W.L., Duncan, B., Houyoux, M., Jang, C., Mathur, R., Odman, T., Xiu, A., 1997. Impact of inert organic nitrate formation on ground-level O₃ in a regional air quality model using the Carbon Bond Mechanism 4. *Geophysical Research Letters* 24, 3205–3208.
- Kumar, N., Odman, M.T., Russell, A.G., 1994. Multiscale air quality modeling: application to southern California. *Journal of Geophysical Research* 99, 5385–5397.
- Liang, J., Jacobson, M.Z., 2000. Effects of subgrid segregation on ozone production efficiency in a chemical model. *Atmospheric Environment* 34 (18), 2975–2982.
- Liu, S.C., Trainer, M., Fehsenfeld, F.C., Parrish, D.D., Williams, E.J., Fahey, D.W., Hübler, G., Murphy, P.C., 1987. Ozone production in the rural troposphere and the implications for regional and global ozone distributions. *Journal of Geophysical Research* 92, 4191–4207.
- Mathur, R., Dennis, R.L., 2003. Seasonal and annual modeling of reduced nitrogen compounds over the eastern United States: emissions, ambient levels, and deposition amounts. *Journal of Geophysical Research* 108 (D15), 4481.
- Mathur, R., Young, J.O., Schere, K.L., Gipson, G.L., 1998. A comparison of numerical techniques for solution of atmospheric kinetic equations. *Atmospheric Environment* 32, 1535–1553.
- Mathur, R., et al., 2004. The multiscale air quality simulation platform (MAQSIP): model formulation and process considerations. Technical Report, Carolina Environmental Program, University of North Carolina at Chapel Hill. <http://cf.unc.edu/cep/empd/pub_files/maqsipnote.pdf> (accessed October 2005).
- Mathur, R., et al., 2005. The multiscale air quality simulation platform (MAQSIP): initial applications and performance for tropospheric O₃ and particulate matter. *Journal of Geophysical Research* 110, D13308.
- North Carolina Department of Environment and Natural Resources (NCDENR), 2004. The North Carolina 8-h O₃ attainment demonstration for various EAC areas. Technical Report prepared by the NCDENR Division of Air Quality for the US EPA Region 4. <http://www.epa.gov/ttnaaqs/ozone/eac/eac_r4.htm> (accessed October 2005).
- Russell, A., Dennis, R., 2000. NARSTO critical review of photochemical models and modeling. *Atmospheric Environment* 34, 2283–2324.
- Sillman, S., Logan, J.A., Wofsy, S.C., 1990. A regional scale model for ozone in the US with subgrid representation of urban and power plant plumes. *Journal of Geophysical Research* 95, 5731–5748.
- Sistla, G., Hogrefe, C., Hao, W., Ku, J.-Y., Zalewsky, E., Henry, R.F., Civerolo, K., 2004. An operational assessment of the application of the relative reduction factors in the demonstration of attainment of the 8-h Ozone National Ambient Air Quality Standard. *Journal of the Air and Waste Management Association* 54, 950–959.
- Sonoma Technology Inc. (STI), 1998. Analyses of meteorological and air quality data for North Carolina in support of modeling. Draft Final Report STI-997420-1818-DFR, prepared for the North Carolina Department of Environment and Natural Resources.
- Steel, R.G.D., Torrie, J.H., Dickey, D.A., 1997. *Principles and Procedures of Statistics: a Biometric Approach*, third ed. McGraw-Hill, New York.
- US EPA, 1991. *Guideline for Regulatory Application of the Urban Airshed Model*, EPA-450/R-91-013. Office of Air Quality Planning and Standards, Research Triangle Park, NC.
- US EPA, 1999. *Draft Guidance on the Use of Models and Other Analyses in Attainment Demonstrations for the 8-h O₃ NAAQS*, EPA-454/R-99-004. Office of Air Quality Planning and Standards, Research Triangle Park, NC.
- US EPA, 2001. *Guidance for Demonstrating Attainment of Air Quality Goals for PM_{2.5} and Regional Haze*. Office of Air Quality Planning and Standards, Research Triangle Park, NC.
- Vukovich, J., Pierce, T., 2002. The implementation of BEIS-3 within the SMOKE modeling framework. In: *Proceedings of the 11th Annual Emissions Inventory Conference: Emissions Inventories—Partnering for the Future*. US Environmental Protection Agency, 15–18 April 2002, Atlanta, GA.